A Method for Efficient Measurement and Reconstruction of Free Form Surfaces Using Vision Guidance

Z. G. Liu[1], Y. F. Li[1] and Paul Bao[2]

[1]City University of Hong Kong, meyfli@cityu.edu.hk, mezgliu@hotmail.com
[2]The Chinese University of Hong Kong, paulbao@ie.cuhk.edu.hk

ABSTRACT

In this paper we present a novel sensor planning method for achieving efficient measurement and reconstruction of freeform object surfaces. Using the modified Bayesian Information Criterion (BIC), we first design a model selection strategy to obtain an optimal model structure for the freeform surface. Based on the selected model structure, we then determine a set of data points to be measured. B-splines are adopted for modeling the free form surface. In order to obtain more reliable parameter estimation for the B-spline model, we analyze the uncertainty of the model and use the statistical analysis of the Fisher information matrix to optimize the locations of the data points needed in the measurements. Using a cloud of data points of a surface acquired by a 3D vision system, we implemented the proposed method for reconstructing freeform surfaces. The experiment results show that the method is effective and promises useful applications in multi-sensor measurements including vision guided CMM for reverse engineering.

Keywords: Sensor planning, 3D reconstruction, B-spline model, freeform surface, 3D vision.

1. INTRODUCTION

Reconstructing the freeform surface from a set of discrete measurement data points is a problem important to many areas including reverse engineering, metrology, inspection by machine vision, computer aided design [1-5]. The first task in the reconstruction of a freeform surface is to obtain the measurement data. Among the various sensing techniques available, mechanical contact probes such as CMM's (Coordinate Measuring Machine) touch probe, and 3D vision systems using structure-light [6] are widely used in practical applications. CMM with touch-triggered probes can provide high measurement accuracy at sub-micron level. However, the measurement speed is much lower than using a 3D vision system. A vision system can acquire thousands of data points over a large spatial range in a snapshot. However, the achievable resolution is relatively lower, at around $100 - 200 \mu m$. Therefore, in practical applications, using one of the techniques means that the user has to suffer from its limitations, e.g. the low speed with CMM.

A way to overcome the limitations of individual sensing technique lies in integrating multiple sensors in the measurement (Fig. 1). Research efforts have been made to achieve this. For example, Nashman et al. [7]

integrated vision in a touch-probe system, where a video camera with a laser triangulation probe and a 3D touch probe were used in a CMM. They presented a cooperative interaction method for the vision and touch-probe system that provides sensory feedback to the CMM for dimension inspection tasks. Chen and Lin [8] presented a vision-aided reverse engineering approach (VAREA) to reconstruct free-form surface models from physical models, with a CMM equipped with a touch-triggered probe and a vision system. The VAREA integrated computer vision, surface data digitization and surface modeling into a single process. The initial vision driven surface triangulation process (IVSTP) generated a triangular patch by using stereo image detection and a constrained Delaunay triangulation method. The adaptive model-based digitization process then refined the surface reconstruction using measurements from the CMM's touch probe. Since the vision system in VAREA used a 3D stereo algorithm to detect 3D surface boundaries, only 3D surface boundaries were reconstructed and geometrical information about the freeform surface could not be retrieved. Recently Shen et al [9, 10] presented a multiple-sensor coordinate measuring system for automated part localization and rapid surface digitization. The multiple-sensor system consists of a high precision CMM equipped with touch

probe and a 3D active vision system. Their research focused on setting up the multiple-sensor system and processing the geometrical information from the vision system. In these systems, the CMM's touch probe plays the role in accurately digitizing a surface, especially when high-precision is desired. How to determine the set of measurement data, including the needed number of the measurement data points and their locations, for accurate reconstruction of freeform surfaces remains untouched [11].
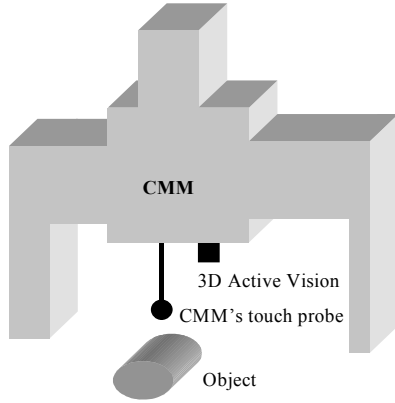
Fig. 1 Multiple-sensor coordinate measuring system

Using a CMM for 3D measurements, only a finite number of discrete measurement data can be taken for a surface. From the statistical viewpoint, each measurement data point contains a certain amount of geometrical information about the surface, and the quantity of information contained in the set of measurement data points depends on the number and locations of the measurement points. Considering the lengthy time needed in using a CMM to take a large number of measurement data points, we should select the locations of the data points to achieve an optimal measurement and reconstruction. Unfortunately, the current practice in using CMM mostly adopts random data point setting on a surface. In such a case, each data point has an equal probability of being picked for the measurement. For example, Woo et al. presented a sampling strategy based on the Hammersley sequence to determine the number of discrete sample points and their locations on a machined surface [12]. Lee [13] proposed a feature based method, which integrates Hammersley sequence and a stratified sampling method, to derive the sampling strategy for various surfaces such as circular, cone, cylindrical, rectangular and spherical surface.

Unlike objects composed of simple geometric primitives, such as planes, lines, spheres and cylinders, freeform surfaces have no obvious features. Therefore, they are more difficult to define and model mathematically than simple geometric objects. In most cases, freeform surfaces are represented by the parametric equations such as Coons patches, B-splines and NURBS (non-uniform rational B-splines). A fundamental question then arises: can we find the parametric model to represent an unknown freeform surface and then select a minimal set of discrete measurement points to obtain these parameters, while controlling the uncertainty of model parameters within a specified tolerance. Here, uncertainty describes the tolerance range within which the unknown true surface lies with some confidence level. The lower the uncertainty of the model, the better the reconstructed surface is. In this paper, we propose a method that allows for optimal measurements and reconstruction of freeform surfaces. Two issues need to be addressed here. The first is how to select the model structure using a cloud of low-precision data acquired by a 3D vision sensor. We use B-splines to represent a freeform surface and present a modified BIC criterion for selecting an optimal model structure for surface representation. The second is how to determine the locations of a set of measurement data points for high-precision measurements e.g. by CMM's touch probe. We analyze the uncertainty of the B-spline model, and use the statistical analysis of the Fisher information matrix to optimize the locations of the measurement data points to minimize the uncertainty of the B-spline model.

The rest of this paper is organized as follows. Section 2 describes the B-splines approximation and model selection for 3D reconstruction of freeform surface. In Section 3, the uncertainty of the B-spline surface is analyzed. Section 4 presents the optimization of the locations of measurement data points. Section 6 gives some experimental results in reconstructing the freeform surfaces of some real objects. Finally, conclusions of the work are given in section 6.

2. B-SPLINE APPROXIMATION AND MODEL SELECTION

2.1 B-spline Approximation
A B-spline surface is defined by the following equation:

$$s(u,v) = \sum_{i=0}^{n_u-1}\sum_{j=0}^{n_v-1} B_{i,p}(u) \cdot B_{j,q}(v) \cdot \phi_{ij} \qquad (1)$$

where n_u and n_v are the number of control points in u and v directions; Φ_{ij}, with $i=0$, 1, …, n_u-1 and $j=0$, 1,…, n_v-1 are the $n=n_u \times n_v$ control points; $B_{i,p}(u)$ for $i=0$, 1, …, n_u-1 and $B_{j,q}(v)$ for $j=0$, 1,…, n_v-1 are the normalized B-

spline of degree p and q for the u and v directions, respectively. The normalized B-spline $B_{i,p}(u)$ and $B_{j,q}(v)$ are defined over the knot vectors $\mathbf{u}=[u_0,u_1,\ldots,u_{n+p}]$ and $\mathbf{v}=[v_0,v_1,\ldots,v_{n+q}]$.

Assume that $(x_k,\ y_k,\ z_k)$ is the coordinates of a measurement point $\mathbf{r}_k$ on the surface, and $(u_k,\ v_k)$ is the location parameters of $\mathbf{r}_k$. Let us further assume that the degrees of p and q and the complete knot vectors $\mathbf{u}$ and $\mathbf{v}$ for surface fitting are also determined. By introducing the measurement point r_k with the corresponding location parameters in Eqn.(1), we have

$$\begin{cases} x_k = \sum_{i=0}^{n_u-1}\sum_{j=0}^{n_v-1} B_{i,p}(u_k)B_{j,q}(v_k)\,x_{ij} \\[2mm] y_k = \sum_{i=0}^{n_u-1}\sum_{j=0}^{n_v-1} B_{i,p}(u_k)B_{j,q}(v_k)\,y_{ij} \\[2mm] z_k = \sum_{i=0}^{n_u-1}\sum_{j=0}^{n_v-1} B_{i,p}(u_k)B_{j,q}(v_k)\,z_{ij} \end{cases} \qquad (2)$$

where $(x_{ij},\ y_{ij},\ z_{ij})$ are the coordinates of the B-spline surface control points Φ_{ij}. Eqn.(2) can be expressed as linear combination of the control points in the B-spline representation. If a total of m points on the surface are considered, we can obtain the least square estimation of $\Phi=[\Phi^T_x,\ \Phi^T_y,\ \Phi^T_z]^T$ of B-spline parameters can then be given as:

$$\begin{cases} \Phi_x = [\mathbf{B^T B}]^{-1}\mathbf{B^T}\cdot\mathbf{X} \\[2mm] \Phi_y = [\mathbf{B^T B}]^{-1}\mathbf{B^T}\cdot\mathbf{Y} \\[2mm] \Phi_z = [\mathbf{B^T B}]^{-1}\mathbf{B^T}\cdot\mathbf{Z} \end{cases} \qquad (3)$$

where $\mathbf{X}=[x_1,x_2,\ \ldots,\ x_m]^T$, $\mathbf{Y}=[y_1,y_2,\ \ldots,\ y_m]^T$ and $\mathbf{Z}=[z_1,z_2,\ \ldots,\ z_m]^T$, the parameters of B-spline model can be represented respectively by

$$\Phi_x = \left[[(x_{ij})_{j=0}^{n_v-1}]_{i=0}^{n_u-1}\right]^T,$$

$$\Phi_y = \left[[(y_{ij})_{j=0}^{n_v-1}]_{i=0}^{n_u-1}\right]^T,$$

$$\Phi_z = \left[[(z_{ij})_{j=0}^{n_v-1}]_{i=0}^{n_u-1}\right]^T,$$

$[\mathbf{B^T B}]^{-1}\mathbf{B^T}$ is the pseudo-inverse matrix of $\mathbf{B}$. $\mathbf{B}$ is a matrix consisting of the tensor products of the B-spline basis functions corresponding to each of the m measurement points on the surface

$$\mathbf{B} = \begin{bmatrix} \overline{B}_{0,0} & \overline{B}_{0,1} & \cdots & \overline{B}_{0,n-1} \\ \overline{B}_{1,0} & \overline{B}_{1,1} & \cdots & \overline{B}_{1,n-1} \\ \vdots & \vdots & \cdots & \vdots \\ \overline{B}_{m-1,0} & \overline{B}_{m-1,1} & \cdots & \overline{B}_{m-1,n-1} \end{bmatrix}$$

and

$$\left|[(B_{i,p}(u_k)\cdot B_{j,q}(v_k))_{j=0}^{n_v-1}]_{i=0}^{n_u-1}\right| = [\overline{B}_{k,0},\ \overline{B}_{k,1},\ldots,\overline{B}_{k,n-1}].$$

2.2 Model Selection

It is known that for a given set of measurement data, there exists a model of optimal complexity that has the smallest prediction/generalization errors for further data. For a B-spline surface, the complexity of the B-spline model is related to the number of its control point (parameter) in u and v directions [14]. If the B-spline model is too complicated, the approximated B-spline surface will tend to over-fit noisy measurement data. If the model is too simple, then it will not be able to fit the measurement data, causing the approximation results to become under-fitted. In general, both over- and under-fitted approximation will have poor generalization capability. Therefore, the problem of finding an appropriate model, referred to as model selection, is important for achieving a high level of generalization capability. The problem of model selection has been studied from various standpoints including information statistics [15], Bayesian statistics [16,17] and structural risk minimization [18]. The Bayesian approach is perhaps the most general and powerful method. Taking the Bayes rules as an axiom, one can calculate exactly the posterior probability of each model. The problem with Bayesian approach lies in the fact that the calculation of these posterior probabilities involves large number of integrations over the parameter space of each model. Usually this is not possible analytically and therefore approximations have to be taken. In fact, all of the other model selection criteria, such as the non-Bayesian BIC, can be viewed as approximations to the Bayesian method. BIC (Bayesian Information Criterion), often known as Schwarz criterion, maximizes

$$BIC = 2L(\Phi:\mathbf{r}) - n\ln(m) \qquad (4)$$

where $L(\Phi:\mathbf{r})$ is the likelihood function for the parameter Φ of the B-spline model, $\mathbf{r}$ is the set of data point, n is the number of control points. It can be seen that BIC has two terms. The first corresponds to the goodness of the fit, whereas the second corresponds to the penalty term for the dimensionality of the model. The higher the dimension of the model, the heavier the penalty.

Consider the likelihood function of the parameter of B-spline model. The pdf $p(r|\mathbf{\Phi})$ of the surface can be factorized into x, y, and z components as

$$p(\mathbf{r}|\mathbf{\Phi}) = p(\mathbf{X}|\mathbf{\Phi}_x) \cdot p(\mathbf{Y}|\mathbf{\Phi}_y) \cdot p(\mathbf{Z}|\mathbf{\Phi}_z) \qquad (5)$$

The residual error sequence is assumed to be zero mean and white Gaussian with variance σ^2. Considering the x component, we have the likelihood function as follows

$$p(\mathbf{X}|\mathbf{\Phi}_x) = \left(\frac{1}{2\pi\sigma_x^2(\mathbf{\Phi}_x)}\right)^{m/2} \exp\left\{-\frac{1}{2\sigma_x^2(\mathbf{\Phi}_x)}\sum_{k=0}^{m-1}[x_k - \mathbf{B}_k\mathbf{\Phi}_x]^2\right\}$$
$$(6)$$

with $\sigma_x^2(\mathbf{\Phi}_x)$ estimated by

$$\hat{\sigma}_x^2(\hat{\mathbf{\Phi}}_x) = \frac{1}{m}\sum_{k=0}^{m-1}[x_k - \mathbf{B}_k\hat{\mathbf{\Phi}}_x]^2 \qquad (7)$$

The likelihood function for component y and z can be obtained in a similar way. Therefore, we can obtain the following BIC criterion for selecting the B-spline model:

$$BIC = \arg\max_{k=1,\dots k_{\max}}\left\{-\frac{m}{2}\sum_{f=x,y,z}\log\hat{\sigma}_{kf}^2(\hat{\mathbf{\Phi}}_{kf}) - \frac{3\log(m)}{2}d_k\right\}$$
$$(8)$$

where m is the number of data points. As the first two terms in equation (8) measure the prediction accuracy of the B-spline model, the BIC criterion will increase as the complexity of the model increases. In contrast, the second term will decrease and act as a penalty for using additional parameters to model the data. However, since the predicted $\hat{\sigma}_{kf}^2$ (f = x, y, z) depends only on the training data sampled for model estimation, they are insensitive when under-fitting or over-fitting occurs. In equation (8), only the second term prevents the occurrence of over-fitting. In fact, an honest estimate of σ_{kf}^2 (f = x, y, z) should be based on a re-sampling procedure. Here, we can divide the available data into a training sample and a prediction sample. The training sample is used only for model estimation, whereas the prediction sample is used only for estimating the prediction data noise σ_{kf}^2 (f = x, y, z). In fact, if the model $\mathbf{\Phi}k$ fitted to the training data is valid, then the estimated variance $\hat{\sigma}_{kf}^2$ (f = x, y, z) from the prediction sample should also be a valid estimate of the data noise.

If the variance $\hat{\sigma}_{kf}^2$ (f = x, y, z) found from the prediction sample becomes unexpectedly large, we have grounds for believing that the candidate model fits the data badly. It is seen that the data noise kf (f = x, y, z)

estimated from the prediction sample is more sensitive to the quality of the model than the one directly estimated from the training sample, as the $\hat{\sigma}_{kf}^2$ (f = x, y, z) estimated from the prediction sample also has the capability of detecting the occurrence of under-fitting or over-fitting.

3. UNCERTAINTY OF B-SPLINE MODEL
The parameter estimation in Eqn.(3) produces estimated values of the parameters. The degree of approximation of B-spline model is related to a number of factors, including the accuracy of the measurements and uncertainty in the B-spline model. It should be noted that all measurement data are contaminated by noise, and it is impossible to find an exact solution for the model. Let's assume that all measurement errors in the three coordinate components are randomly and independently sampled from a normal distribution with zero mean and variance σ^2. Eqn.(3) gives the maximum likelihood of the estimate $\hat{\mathbf{\Phi}}$ of the true model $\mathbf{\Phi}$. The estimated parameter errors $\mathbf{\Phi} - \hat{\mathbf{\Phi}}$ are distributed as multi-variable normal distribution with zero mean and covariance

$$\mathbf{C} = \sigma^2\begin{bmatrix} (\mathbf{B}^T\mathbf{B}) & \mathbf{0} & \mathbf{0} \\ \mathbf{0} & (\mathbf{B}^T\mathbf{B}) & \mathbf{0} \\ \mathbf{0} & \mathbf{0} & (\mathbf{B}^T\mathbf{B}) \end{bmatrix}^{-1} = \sigma^2\mathbf{M}^{-1} \qquad (9)$$

The presence of random errors in the inverse solution is an indication of its inherent uncertainty in the B-spline model parameters. Considering the following quadratic form

$$(\mathbf{\Phi} - \hat{\mathbf{\Phi}})^T\mathbf{C}^{-1}(\mathbf{\Phi} - \hat{\mathbf{\Phi}}) = \frac{1}{\sigma^2}(\mathbf{\Phi} - \hat{\mathbf{\Phi}})^T\mathbf{M}(\mathbf{\Phi} - \hat{\mathbf{\Phi}})$$
$$(10)$$

that defines the shape of the normal parameter error distribution. In fact, the quadratic form defines a hyper-ellipsoid on which the true model must lie. We do not know the position of this surface as we do not know the value of $\mathbf{\Phi}$. However, we know the range within which the unknown true $\mathbf{\Phi}$ value lies with a confidence interval. For a confidence level γ, we can find from the distribution a number χ_γ^2 for which there is a probability

$$\frac{1}{\sigma^2}(\mathbf{\Phi} - \hat{\mathbf{\Phi}})^T\mathbf{M}(\mathbf{\Phi} - \hat{\mathbf{\Phi}}) < \chi_\gamma^2$$

for γ such that

It follows that there is also a probability for γ that gives the hyper-ellipsoid

$$(\mathbf{\Phi} - \hat{\mathbf{\Phi}})^T\mathbf{M}(\mathbf{\Phi} - \hat{\mathbf{\Phi}}) = \sigma^2\chi_\gamma^2 \qquad (11)$$

The true model will be contained in the above ellipsoid which is referred to as the ellipsoid of confidence. The ellipsoid of confidence gives us a useful visual image of the uncertainty of parameter $\mathbf{\Phi}$ of the B-spline surface. In Eqn.(9)-(11), $\mathbf{M}$ is also known as the Fisher information matrix which characterizes the uncertainty in the estimated parameters. Therefore, the problem of selecting optimal set of measurement data for high-precision measurement for CMM is to find the locations of the measurement data points for which the estimation uncertainty is minimized in some sense. Various criteria exist for optimizing the Fisher information matrix to achieve minimum estimation errors. The major criteria includes *Cond*($\mathbf{M}$), *Trace*($\mathbf{M}$) (A-optimality), the maximum eigenvalue of $\mathbf{M}^{-1}$ (E-optimality), and *Det*($\mathbf{M}$) (D-optimality) [19]. From the standpoint of Shannon entropy, these criteria measure the amount of information contained in the probability distribution representing the parameter errors. Thus, ensuring that the important and necessary information in the B-spline model is embodied in the measurement data set is the primary concern in selecting optimal set of measurement data for high-precision measurements for CMM. Here the optimal criterion adopted is the D-optimality, or the determinant criterion, for which the determinant of the Fisher information matrix $|\mathbf{M}|$ is to be maximized. Geometrically, The volume of the ellipsoid is inversely proportional to the square root of the determinant $|\mathbf{M}|$. A large $|\mathbf{M}|$ corresponds to a small volume of the model parameter space, indicating that the true parameters are well localized and that the knowledge or information we have about them is highly reliable [20]. Here, we define $|\mathbf{M}|$ as the uncertainty measurement for the estimated parameter vector $\mathbf{\Phi}$.

4 OPTIMIZING MEASUREMENTS

As the uncertainty of a B-spline model is dependent on the number and locations as well as the variance of the measurement data, the sensing strategy plays a critical role in the measurement and reconstruction results. A sensing strategy should be able to determine the number of measurement data to sample and the locations to take the measurements, while maintaining the uncertainty of the reconstructed B-spline model sufficiently low.

4.1 Determining the Number of Measurement Data

Since the reconstruction of a freeform surface is based on the measurements at discrete points to be sensed by a CMM's touch probe, these discrete points must contain sufficient information that allows the freeform surface to be reconstructed. However, the number of measurement

data has to be limited, to achieve a reasonable speed in the measurement process. From the statistical point of view, the number of measurement data should be at least ten times the number of the parameters in the B-spline model to make the B-spline regression analysis statistically meaningful. For example, for a bi-cubic B-spline model with $h \times l$ B-spline basic functions, the number of parameters is $(h+3) \times (l+3)$. Therefore, at least $10 \times (h+3) \times (l+3)$ measurement data are required.

4.2 Optimizing the Locations of Measurement Data

Since $|\mathbf{M}|$ is dependent not only on the number of measurement data, but also on the locations of measurement data, we should also optimize the locations of the measurement data to maximize $|\mathbf{M}|$. The spatial locations of the measurement data on the freeform surface then constitute the design variables. Each candidate measurement data point can vary its location within a specified surface. Thus, the location of a measurement data point is represented by two parameter variables (u, v) for surface parameterization. The coordinate (x, y, z) of the measurement data can be obtained from the parameter variables (u, v) with appropriate coordinate transformations. Thus, optimizing the locations of measurement data points for minimizing the uncertainty of a B-spline model can be stated as follows:

$$\max_{u_k, v_k} |\mathbf{M}|$$

Subject to: $(u_k, v_k) \in [0,1]$, $k=0,1,\dots m\text{-}1$. $\qquad$ (12)

The problem is essentially a combinatory optimization problem. Since the objective function $|\mathbf{M}|$ is non-smooth and nonlinear, the existence of the derivations at all points is not guaranteed. This makes the optimization difficult if using a standard optimization method. To simplify the problem, the $|\mathbf{M}|$ can be evaluated with an existing discrete D-optimal design method called Fedorov exchange algorithm. This algorithm implements an efficient neighborhood search for the maximum determinant of the Fisher information matrix $\mathbf{M}$.

Consider the incremental form of $|\mathbf{M}|$. Each additional measurement data incrementally update $\mathbf{M}$, so that after $k+1$ measurements, its value becomes

$$\mathbf{M}(k+1) = \mathbf{M}(k) + \mathbf{H}_k^T \mathbf{H}_k.$$

The corresponding determinant of $\mathbf{M}$ then is

$$|\mathbf{M}(k+1)| = (1 + \mathbf{H}_{k+1} \cdot \mathbf{M}^{-1}(k) \cdot \mathbf{H}_{k+1}^T) \cdot |\mathbf{M}(k)|$$

$$(13)$$

where $\mathbf{H}_k = [\mathbf{B}_{k+1}, \mathbf{B}_{k+1}, \mathbf{B}_{k+1}]$, $\mathbf{B}_{k+1}$ is the basis function vector evaluated at location (u_{k+1}, v_{k+1}).

If a point is to be removed from the set of sample points, all the addition and subtraction signs in Eqn.(13) are reversed. To evaluate $|\mathbf{M}|$ by Fedorov exchange algorithm, each point in the set of measurement data is considered for exchange with each of the available candidate point. The pair of points chosen to exchange is the pair that maximizes the increase in the determinant of $\mathbf{M}$. This process is repeated until no further increase in the determinant can be obtained by the exchange.

If we denote the point to be added by $\mathbf{H}_+$, and the point to be replaced by $\mathbf{H}_-$, then by exchanging the pair of $\mathbf{H}_+$ and $\mathbf{H}_-$, the new determinant is

$$|\mathbf{M} + \mathbf{H}_+^T \mathbf{H}_+ - \mathbf{H}_-^T \mathbf{H}_-| = |\mathbf{M}| \cdot [1 + \Delta(\mathbf{H}_+, \mathbf{H}_-)]$$

(14)

where

$$\Delta(\mathbf{H}_+, \mathbf{H}_-) = \mathbf{H}_+ \mathbf{M}^{-1} \mathbf{H}_+^T - \mathbf{H}_- \mathbf{M}^{-1} \mathbf{H}_-^T (1 + \mathbf{H}_+ \mathbf{M}^{-1} \mathbf{H}_+^T) + (\mathbf{H}_+ \mathbf{M}^{-1} \mathbf{H}_-^T)^2$$

(15)

It is obvious from Eqns.(14) and (15) that it is critical for Fedorov exchange algorithm to find a candidate point to replace a point in the current measurement data set in turn, which maximizes $\Delta(\mathbf{H}_+, \mathbf{H}_-)$.

In this work, we use simulated annealing algorithm to search the candidate point. Simulated annealing (SA) is a random search algorithm that is popular for solving both continuous and discrete global optimization problem. The optimal procedure using discrete SA algorithm for optimization of the locations of the measurement data point can be stated briefly as follows:

Step 1. Select a measurement point $r_k(u_k, v_k) \in S$, $k = 0, 1, \ldots m\text{-}1$ from the set of sample points.

Step 2. Generate a candidate point $r_c(u_c, v_c) \in S$ according to a specified generator.

Step 3. Set

$$r_k(u_k, v_k) = \begin{cases} r_c(u_c, v_c) & if\ \Delta(\mathbf{H}_+, \mathbf{H}_-) > 0 \\ r_c(u_c, v_c) & with\ probability\ p\ if\ \Delta(\mathbf{H}_+, \mathbf{H}_-) < 0 \\ r(u_k, v_k) & otherwise \end{cases}$$

(16)

where p is the probability of accepting p when $\Delta(\mathbf{H}_+, \mathbf{H}_-) < 0$. For simplicity, the probability p is set as constraint.

Step 4. Repeat Step 2 and 3 until the stopping criterion is satisfied.

Step 5. Select another measurement data point from the sample set, and repeat step 1 to 4 until all measurement data in the selected measurement are exchanged.

5. EXPERIMENTS

To demonstrate the effectiveness of the proposed sensor planning strategy for reconstructing freeform surfaces, two experiments are conducted. In the current implementation, uniform cubic B-spline model is used to represent these surfaces.

The first example we chose for experiment is to reconstruct the surface of a computer. To reconstruct the freeform surface, the first thing is to determine the control point number n_u and n_v in the u and v parameter directions. A 3D vision system was used to acquire a cloud of data points on the mouse surface. The vision system consisting of a laser stripe projector and CCD camera measures 3D coordinates based triangulation. Then, we used our modified BIC Criterion to select B-spline model structure (n_u and n_v) to represent the freeform surface.

To demonstrate the effectiveness of the modified BIC criterion, we compared it with the BIC and cross validation (CV) methods respectively. The two following performance indices were used:

1) model complexity, which refers to the number d ($d = n_u \times n_v$) of control points of a B-spline model determined by a given model selection criterion.

2) estimation accuracy, which is defined as the MSE (mean square error) between the actual data points and the regression estimate chosen by a given model selection method.

In this section, we use box plots of the MSE and model complexity of each method to test the performance of different model selection methods. The experiments with different sample sizes were designed to observe the differences between the different model selection methods. For each sample size, the sample points were selected randomly from the 'data cloud' acquired by the 3D vision system, and then used to determine the structure of the B-spline model with a different selection criterion. The above selection process was repeated 100 times. The comparison results are presented in box plots which give the empirical distribution of the comparison based on 100 iterations in the model selection. Evaluation results with a set of 300 are shown as a box plot.
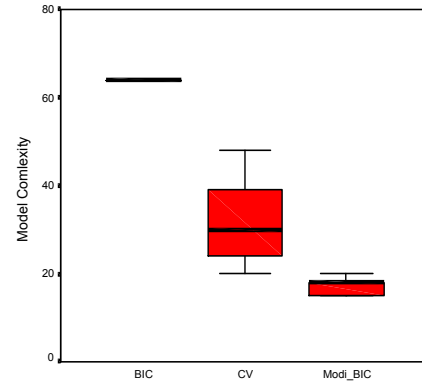
(a) model complexity

(b) Estimation accuracy
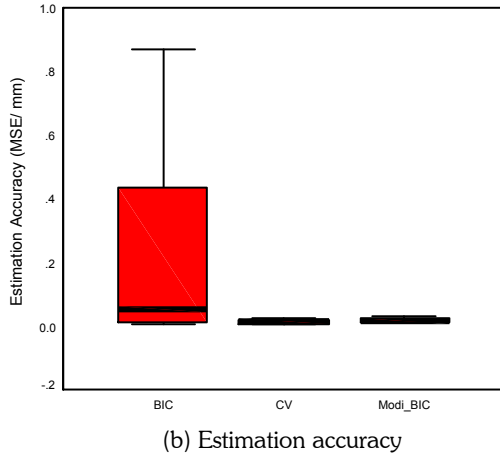
Fig. 2. Results of Model selection with 300 training samples and 200 prediction samples.

Fig. 3. The locations of the measurement data after optimization

By our method, a model structure with 5 control points in both u and v directions (totally 25 parameters to be estimated) was selected as the optimal model structure. The minimal set of 250 measurement data was used to estimate these parameters. As discussed in section 3, high uncertainty in the estimated parameters indicates that the estimated values of $\hat{\Phi}$ can deviate significantly from the true values of Φ. In other words, the lower the uncertainty in the estimated parameters, the more reliable the estimation $\hat{\Phi}$ is.

By our method, a model structure with 5 control points in both u and v directions (totally 25 parameters to be estimated) was selected as the optimal model structure. The minimal set of 250 measurement data was used to estimate these parameters. As discussed in section 3, high uncertainty in the estimated parameters indicates that the estimated values of $\hat{\Phi}$ can deviate significantly from the true values of Φ.

Next, we employed the Fedorov exchange algorithm to optimize the locations of the measurement data. we use the $\log(|\mathbf{M}|)$ as the indicator of the uncertainty in a B-spline model. The larger the $\log(|\mathbf{M}|)$, the lower the uncertainty. The locations after the optimization are shown in figure 3. Here an interesting phenomenon to note on the optimized locations of the measurement data is that after optimization, the measurement data are located in the neighbor of each model parameter. These relocations allow for more reliable model estimation in the parameterization field. The coordinates (x, y, z) of the measurement data can be mapped from the parameter variables (u, v) with appropriate coordinate transformations.

It is observed that after optimization of the locations of the measurement data, the uncertainty of the B-spline model is significantly reduced compared with using random locations in the measurement data. The uncertainty of a B-spline model can also be reduced by increasing the sample size. To achieve the same level of uncertainty in the B-spline model with random locations in the measurement data, about 310 more measurement data would be needed in the sample set. This allows a much more reliable model estimation to be obtained by optimizing the locations of the measurement data point to be sensed by CMM's touch probe without increasing the number of measurements to be taken.
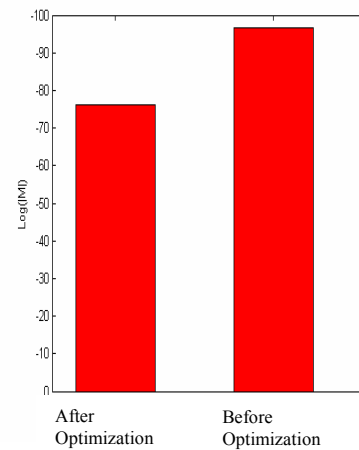
Fig. 4. The uncertainty of the B-spline models before and after optimization

From the experiments, we observed that in the parameterization fields, the locations of the measurement data points are related to the structure of the B-spline

model. For a uniform cubic B-spline model, the control points are distributed uniformly in the u and v directions, giving rise to some clusters in which the measurement data points are located. Therefore, we infer that the structure of a B-spline model determines the locations of the measurements and the model structure represents the geometrical feature of a surface which can be extracted from the cloud of data acquired by a vision system.

ACKNOWLEDGEMENT

7. REFERENCES

[1] P. Chivate and A. Jablockow, Review of Surface Representations and Fitting for Reverse Engineering, *Computer Integrated Manufacturing Systems*, Vol. 18, No. 3, 1995, pp. 193-204.

[2] C. Song and S. Kim, Reverse Engineering: Autonomous Digitization of Free-form Surfaces on a CNC Coordinate Measuring Machine, *International Journal of Machine Tools and Manufacturing*, Vol. 37, No. 7, 1997, pp. 1041-1051.

[3] W. Thompson and J. Owen, Feature-based Reverse Engineering of Mechanical Parts, *IEEE Trans. Robotics and Automation*, Vol. 15, No. 1, 1999, pp. 57-66.

[4] W. Wolovich, H. Albakri, and H. Yalcin, The Precise Measurement of Free-form Surface, *Trans. of AMSE, Journal of Manufacturing Science and Engineering*, Vol. 124, No. 2, 2002, pp. 326-332.

[5] D. Weir, M. Milroy, C. Bradley, and G. Vickers, Wrap-around B-spline Surface Fitting to Digitized Data with Application to Reverse Engineering, *Trans of ASME, Journal of Manufacturing Science and Engineering*, Vol. 122, No.2, 2000, pp. 323-330.

[6] Y. F. Li and R. S. Lu, Uncalibrated Euclidean 3D Reconstruction Using an Active Vision System, *IEEE Transactions on Robotics and Automation*, Vol. 20, No. 1, Feb. 2004, pp. 15-25.

[7] M. Nashman, T. Hong, W. Rippey, and M. Herman, An Integrated Vision Touch-probe System for Dimension Inspection Tasks, In *Proc. SME Applied Machine Vision'96 Conference*, Cincinnati, OH. 1996, Society of Manufacturing Engineers, pp. 243-255.

[8] L. Chen and G. Lin, A Vision-aided Reverse Engineering Approach to Reconstructing Free-form Surfaces, *Robotics and Computer-integrated Manufacturing*, Vol. 13, No. 4, 1997, pp. 323-336.

[9] T. Shen, J. Huang, and C. Menq, Multiple-sensor Integration for Rapid and High-precision Coordinate Metrology, *IEEE/ASME Trans. Mechatronics*, Vol. 5, No. 2, 2000, pp. 110-121.

[10] T. Shen, J. Huang, and C. Menq, Multiple-sensor Planning and Information Integration for Automatic Coordinate Metrology, *Journal of Computing and Information Science in Engineering*, Vol. 1, 2001, pp. 167-179.

[11] Y. F. Li and Z. Liu, Uncertainty-Driven Viewpoint Planning for 3D Object Measurements, *Proc. IEEE International Conference on Robotics and Automation*, Taipei, Taiwan, Sept. 2003, pp.127-132.

[12] T. Woo and R. Liang, Dimensional Measurement of Surfaces and Their Sampling, *Computer-Aided Design*, Vol. 25, No. 4, 1993, pp. 233-239.

[13] G. Lee, J. Mou, and Y. Shen, Sampling Strategy Design for Dimensional Measurement of Geometric Feature Using Coordinate Measuring Machine, *International Journal of Machine Tools and Manufacture*, Vol. 37, No. 7, 1997, pp. 917-934.

[14] Z. Yan, B. Yang, and C. Menq, Uncertainty Analysis and Variation Reduction of Three Dimensional Coordinate Metrology. Part I: Geometric Error Decomposition, *International Journal of Machine Tools and Manufacture*, Vol. 39, No. 8, 1999, pp. 1199-1217.

[15] M. Sugiyama and H. Ogawa, Subspace Information Criterion for Model Selection, *Neural Computation*, Vol. 13, No. 8, pp. 1863-1889, 2001.

[16] G. Shwartz, Estimating the Dimension of a Model, *Annals of Statistics*, Vol. 6, 1978, pp. 461-464.

[17] P. Torr, Bayesian Model Estimation and Selection for Epipolar Geometry and Generic Manifold Fitting, *Int'l. J. Computer Vision*, Vol. 50, No. 1, 2002, pp. 35-61.

[18] V.cherkassky, X.Shao, F. Mulier, and V. Vapnik, Model Complexity Control for Regression Using VC Generalization Bounds, *IEEE Trans. Neural Networks*, Vol. 10, No. 5, 1999, pp. 1075-1089.

[19] W. Chio and T. Kurfess, Uncertainty of Extreme Fit Evaluation for Three Dimensional Measurement Data Analysis, *Computer-Aided Design*, Vol. 30, No. 7, 1995, pp. 549-557.

[20] P. Whaite and F. Ferrie, Autonomous Exploration: Driven by Uncertainty, *IEEE Trans. Pattern Analysis and Machine Intelligence*, Vol. 19, No. 3, 1997, pp. 193-205.